2
Mathematical formulations

The problem of modelling the torsional dynamics of a flexible shaft can be approached in different ways. From that, only two different models were studied in this thesis, one with concentrated parameters, the other a 2 DOF torsional mass-spring system considering only the mechanical part of the top drive motor (fig. 2.1).

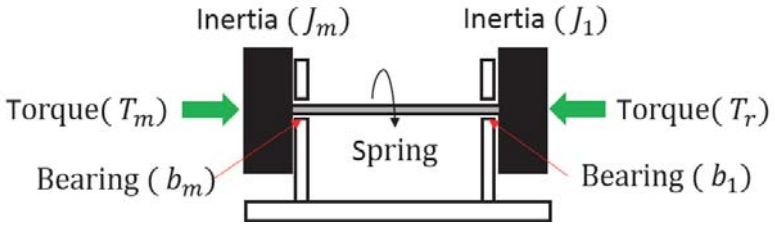

Figure 2.1: 2DOF mechanical system

This model can provide fast simulations with a good description of the problem, it is also used as the reference model for Model Reference Adaptive Controllers i.e. MRAC without compromising computational effort. The model was written in state-space form with the A matrix and the state vector x described in eq.(2.1).

$$A = \begin{bmatrix} \frac{-b_1}{J_1} & \frac{K}{J_1} & 0 \\ -1 & 0 & 1 \\ 0 & \frac{-K}{J_m} & \frac{-b_m}{J_m} \end{bmatrix} \quad B = \begin{bmatrix} \frac{-Tr}{J_1} \\ 0 \\ \frac{T_m}{J_m} \end{bmatrix} \quad x = \begin{bmatrix} \dot{\theta_1} \\ \theta_m - \theta_1 \\ \dot{\theta_m} \end{bmatrix} \tag{2.1}$$

where the dynamics equation is:

$$\dot{x} = Ax + B \tag{2.2}$$

and b_1 is the bearing friction on the inertia J_1, and J_1 the moment of inertia of the rotor. K, is the drill string torsional constant, T_m and T_r are the torque on the motor and the reaction torque, b_m is the bearing viscous friction on the motor, and J_m is the motor inertia . $\dot{\theta_m}$ is the angular speed of the motor and $\dot{\theta_1}$ is the angular speed of J_1.

The DC motor (fig. 2.2) is modeled by the equations of the mechanical Eq.(2.3) and electrical parts Eq.(2.4) as well as the torque constant k_t that is the relation between T_m and i.

All the parameters used for the motor were obtained by [3] from the test rig.

$$J_m \frac{d^2\theta}{dt^2} = T_m - b_m \frac{d\theta}{dt} \tag{2.3}$$

$$L\frac{di}{dt} = -Ri + V - e \tag{2.4}$$

where i is the electrical current in amperes, R is the resistance in ohms, L is the inductance in Henry, V is the voltage, and e the back emf, that is proportional to the angular velocity of the shaft by a constant factor Ke.

$$e = K_e\dot{\theta} \tag{2.5}$$

Then, we can introduce the motor dynamics 2.3 and 2.4 in the state space of the 2DOF mechanical system 2.1 to obtain a better state space representation of the system and therefore a 3 DOF sytem. Where the dynamics equation is:

$$\dot{x} = Ax + Bu \tag{2.6}$$

where u is the input vector, and the state matrix A and vector B are:

$$A = \begin{bmatrix} 0 & 1 & 0 & 0 & 0 \\ \frac{-K}{J_m} & \frac{-(b_m+D_{il})}{J_m} & \frac{K}{J_m} & \frac{D_{il}}{J_m} & \frac{k_t}{J_m} \\ 0 & 0 & 0 & 1 & 0 \\ \frac{K}{J_1} & \frac{D_{il}}{J_1} & \frac{-K}{J_1} & \frac{-D_{il}}{J_1} & 0 \\ 0 & 0 & 0 & \frac{-K_eN}{L} & \frac{-R}{L} \end{bmatrix} \quad B = \begin{bmatrix} 0 \\ 0 \\ 0 \\ 0 \\ \frac{1}{J_1} \end{bmatrix} \quad x = \begin{bmatrix} \theta_m \\ \dot{\theta_m} \\ \theta_1 \\ \dot{\theta_1} \\ i \end{bmatrix} \tag{2.7}$$

where D_{il} is the damping from internal losses of the drill string, K_e is the DC motor speed constant, and N is the gearbox attached to the motor relation.

The second model is a 20 DOF Lumped parameters flexible shaft (fig. 2.3), that was used to obtain a more complete and therefore more complex model of the system. This model also uses a DC motor model with electrical and mechanical parts, modeling this way the dynamics of the DC motor.

In the lumped parameters model (fig.2.3), each element or DOF is an elemetary inertia-damper-spring system modeled as:

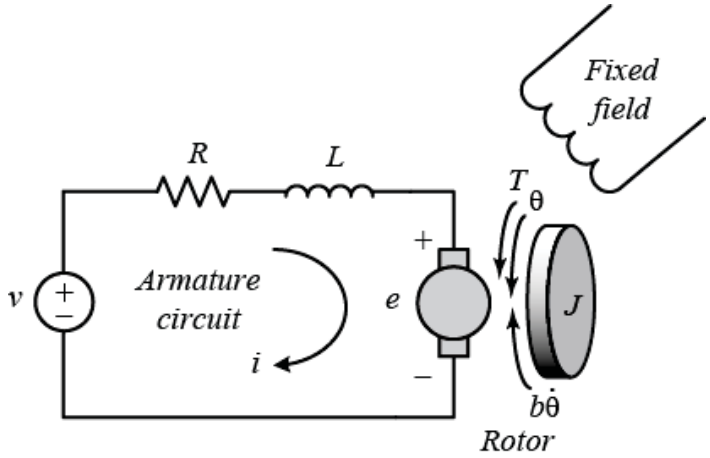

Figure 2.2: DC Motor scheme - *Image from The MathWorks, Inc.*

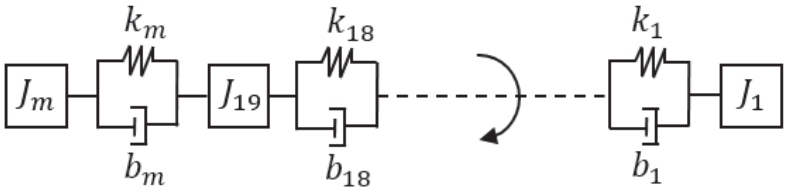

Figure 2.3: Lumped parameters flexible shaft

$$I\frac{d^2\theta}{dt^2} = -k\theta - b\frac{d\theta}{dt} \tag{2.8}$$

Writing the differential equations in (2.8) for each sub system and assembling them in a matrix form it becomes:

$$\bar{M}\ddot{\theta} + \bar{B}\dot{\theta} + \bar{K}\theta = \bar{\tau} \tag{2.9}$$

where $\bar{\theta}$ is the state vector representing the angular displacements of the lumped masses, $\bar{\tau}$ is the external torques vector, the system mass matrix $\bar{M}$, the damping matrix $\bar{B}$, and the spring matrix $\bar{K}$ are:

$$\bar{M} = \begin{bmatrix} J_1 & & & & \\ & J_2 & & & \\ & & \ddots & & \\ & & & J_{19} & \\ & & & & J_m \end{bmatrix} \tag{2.10}$$

$$\bar{B} = \begin{bmatrix} b_1 & -b_1 & & & \\ -b_1 & (b_1+b_2) & -b_2 & & \\ & -b_2 & \ddots & & \\ & & & (b_{18}-b_m) & -b_m \\ & & & -b_m & b_m \end{bmatrix} \tag{2.11}$$

$$\bar{K} = \begin{bmatrix} k_1 & -k_1 & & & \\ -k_1 & (k_1+k_2) & -k_2 & & \\ & -k_2 & \ddots & & \\ & & & (k_{18}-k_{19}) & -k_{19} \\ & & & -k_{19} & k_{19} \end{bmatrix} \tag{2.12}$$

This way, the mechanical lumped parameters of the drill string can be written substituting (2.11) and (2.12) in (2.9).

2.1 Torque on bit formulation

The contact between bit and rock is modeled, according to Armstrong [4] by the sum of a Coulomb static friction coefficient, a dynamic coefficient and a viscous friction, dependent of the angular speed. This contact appears in the model on the inertia J_1.

$$T_r = (T_C + (T_{brk} - T_C) \cdot exp(-c_v|\omega|))sign(\omega) + f\omega \qquad if|\omega| \geq \omega_{th} \tag{2.13}$$

and:

$$T_r = \omega \frac{(f\omega_{th} + (T_C + (T_{brk} - T_C) \cdot exp(-c_v\omega_{th})))}{\omega_{th}} \qquad if|\omega| < \omega_{th} \tag{2.14}$$

where: T_r is the friction torque, T_C is the Coulomb friction torque, T_{brk} is the static friction torque, c_v is the dynamic friction coefficients, ω is the angular speed, f is the viscous friction coefficient and ω_{th} is the velocity of threshold that is in the order of 10^{-4} included to avoid numerical problems.

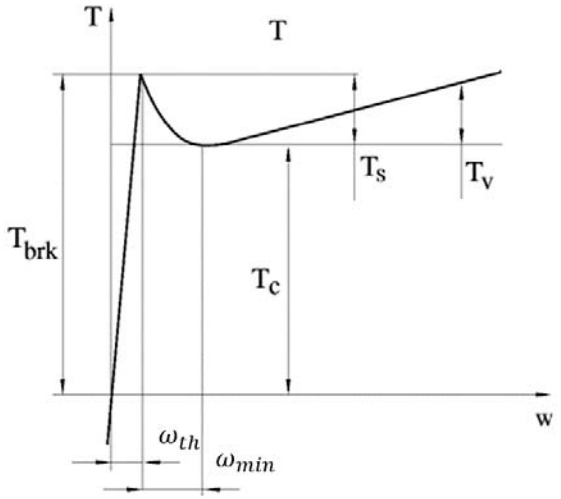

Figure 2.4: Friction torque by angular speed

2.2 Stick-Slip

Stick-slip is a phenomenon that has an important role in different areas of engineering. It is the main source of noise in car breaking systems. It is heavily associated with earthquakes, as it is one of the main sources of seismic incidents, as the rock becomes distorted, or bent, but holds its position until the earthquake occurs. When the rock snaps back into an unstrained position it is called elastic rebound. Stick-slip displacement on a fault radiates energy in the form of seismic waves, creating an earthquake.

And, the focus of this thesis, is one of the major failures cause in drilling for oil. The stick-slip vibration phenomenon has become an important risk element to be evaluated in the planning of oil and gas well drilling. the reason for this is the widespread use of new, highly efficient drill bits using polycrystaline diamond cutters (PDC) that cut the rock by shear rotary force compared to the previous roller-cone bits that crushed the formations and required only a limited amount of energy to turn.

The stick-slip action is characterized by a relatively slow absorption and fast release of energy and its main origin is the difference between a bigger static and a lower dynamic friction coefficient. In drilling, the drillstring can accumulate energy during several complete rotations before the slip begins. When that happens, the angular speed of the drill can achieve more than 4 times the desired speed, many times leading to failure of components.

In the slip or release phase, the string spins out of control and this is what creates stick-slip-associated destructive vibrations. Stick-slip occurring

where the PDC cutters meet the rock has the potential to create the longest stick and most violent slip periods.

Stick-slip can also be produced by the friction between the hole wall and the drill-string itself, specially in horizontal wells where the gravity pulls the drillstring against the formation. In this interface, there is no potential for holding up the rotation for a long stick period and the stick-slip from friction is typically less threatening, but also requires attention as it contributes to torsional vibrations in the column.

In next two sections simple dynamical problems are presented as an introduction to how the stick-slip happens and its characteristics to allow a better understanding of this complex phenomenon to later develop the simulations of the rotational drilling problem.

2.2.1 One cart mass-spring-damper system stick-slip

The most common stick-slip problem in literature is the one happening on a linear 1 degree of freedom (DOF) mass-spring-damper system where the mass is positioned over a moving belt (fig.2.5) This model is presented to clarify the dynamics of the stick-slip movement on a simple system.

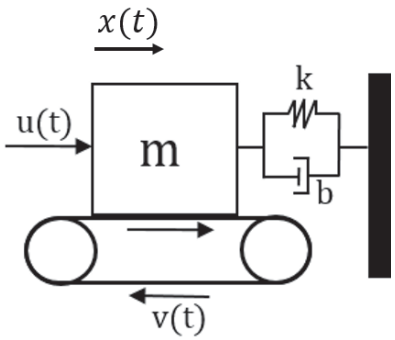

Figure 2.5: 1 DOF linear stick-slip

Where m is the mass, k is the spring constant, b is the damper coefficient, $v(t)$ is the speed of the belt and $u(t)$ is a control force that may act on the system. $x(t)$ is the position of the mass and $\dot{x}(t)$ is the mass speed relative to the ground. The dynamics of this system can be written as:

$$m\ddot{x} + b\dot{x} + kx = F_r + u(t) \tag{2.15}$$

The contact force between the mass and the belt is modeled as:

$$F_r = (F_C + (F_{brk} - F_C) \cdot exp(-c_v|v|(t)|))sign(v) + \mu v \qquad if \quad |v| \geq v_{th} \tag{2.16}$$

and

$$F_r = v\frac{(fv_{th} + (F_c + (F_{brk} - F_c) \cdot exp(-c_v v_{th})))}{v_{th}} \qquad if \quad |v| < v_{th} \qquad (2.17)$$

where: F_r is the friction force, F_C is the Coulomb friction force, F_{brk} is the static friction force, c_v is the dynamic friction coefficient, $\dot{y}(t)$ is the relative speed between the mass and the belt, and μ is the viscous friction coefficient.

This system was then simulated in open loop (no control input $u(t)$) using parameters from tab. 2.1, with the velocity of the belt $v(t)$ being constant. The results for the linear displacement of the mass and the velocity of the mass in reference to the ground are shown in (fig. 2.6(a) and 2.6(b))

Parameter	**Value**	**Unit**
Breakaway friction force (F_{brk})	7	N
Coulomb friction force (F_c)	0.47	N
Mass (m)	0.7	kg
Damper (b)	1	$\frac{N}{m/s}$
Spring (k)	21.6	$\frac{N}{m}$
Speed of the belt (v)	0.061	$\frac{m}{s}$

Table 2.1: 1DOF model parameters

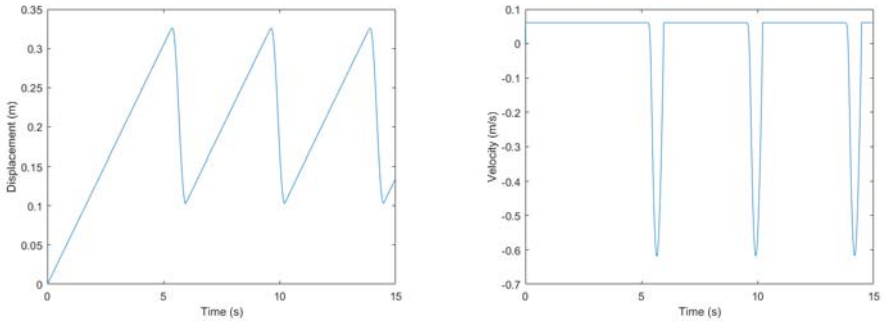

2.6(a): 2.6(b):

Figure 2.6: Simulation results for the 1 DOF linear system: (a) Displacement in m and (b) Velocity in m/s

On the displacement graph (fig. 2.6(a)) one can see the characteristic periodic stick-slip phenomenon where the sections of the curve banked to the right are the stick phases and the almost vertical regions are the slip

The phase plot speed vs. displacement of this system, ploted in (fig. 2.7), shows a line starting from left with constant speed representing the energy accumulation of the mass in contact with the belt, an then a "D" shaped curve representing the periodic stick-slip oscillations of the mass on top of the constant speed belt.

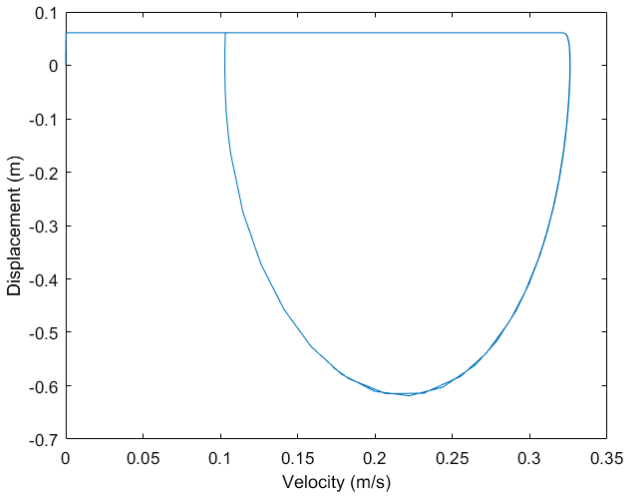

Figure 2.7: Phase plot of the 1 DOF linear system

With the basics of the stick-slip movement presented, the next section (2.3) will describe the stick-slip movement of a rotational system.

2.3 Rotational stick-slip system

The stick-slip also occurs in rotational motion, like the one in drilling systems. In every rotational system where different flexible bodies, with different angular velocities become in contact there may be the appearance of stick-slip. The study of stick-slip in rotational motion systems will focus in this thesis on the drilling problem, where the system shown in fig. 2.8 is simulated to analyze the influence of friction laws on the behavior of the system.

In the simulation results presented in this section all graphs show in blue the angular speed of the Bit, and in green the angular speed of the top drive motor. Simulations were performed using the 20DOF lumped parameters model presented on section 2 for the drillstring.

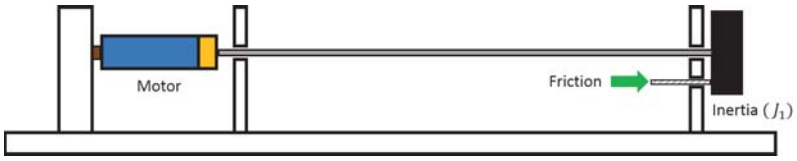

Figure 2.8: Rotational stick-slip model

This system was simulated with the Motor being an infinite torque source with controlled RPM. The friction law used is the one shown in section 2.1 and the initial values of the parameters are shown in Table 2.2

Parameter	Value	Unit
Breakaway friction coefficient (μ_{brk})	0.5	–
Coulomb friction coefficient (μ_c)	0.47	–
Normal force on Bit (N_f)	26	N
Viscous friction coefficient (b)	0.001	$\frac{Nm}{rad/s}$

Table 2.2: Friction parameters

Table 2.3 show the mechanical and electrical parameters used in this simulations.

Parameter	Value	Unit
String length (L)	1.7	m
String diameter (mm)	3	mm
Total inertia of $J_1(J_1)$	0.01555819	kgm^2
String stiffness (K)	0.2548	Nm/rad
Moment of inertia of motor (J_m)	0.37×10^{-3}	kgm^2
Armature inductance (L_{DC})	1.10×10^{-3}	H
Armature resistance (R_{DC})	0.33	Ω
Torque constant (K_t)	0.12	Nm/A
Speed constant (K_e)	6.02×10^{-2}	$V/(rad/s)$

Table 2.3: Simulation parameters

The simulation with this set of parameters, and the speed of top drive being constant $V_{TD} = 2(rad/s)$ results in the stick-slip behavior shown in fig. 2.9

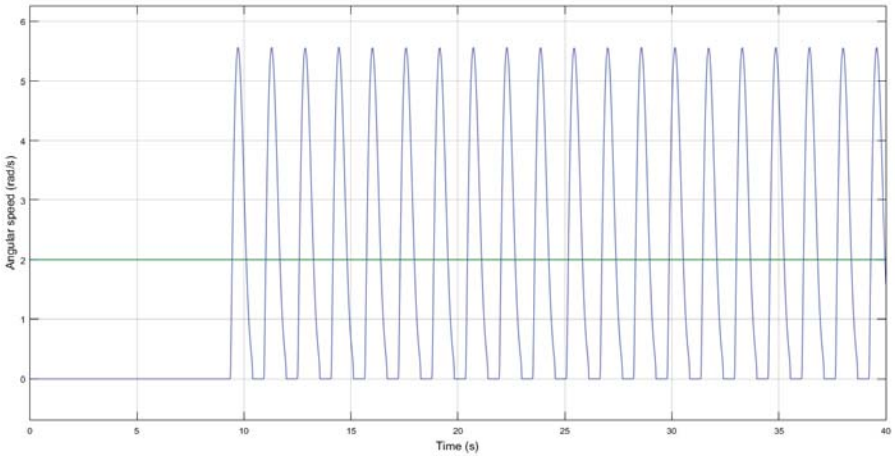

Figure 2.9: Simulation with parameters from Table 2.2

Next, we simulate the same system with the Coulomb friction coefficient $\mu = 0.48$ and as one can see in fig. 2.10, there is no longer stick slip, after the energy accumulation on the torsional spring in the beginning of the simulation, the bit breaks loose but now, with this slightly increase of the Coulomb friction

coefficient the bit stabilizes at the same speed of the top drive after a few oscillations.

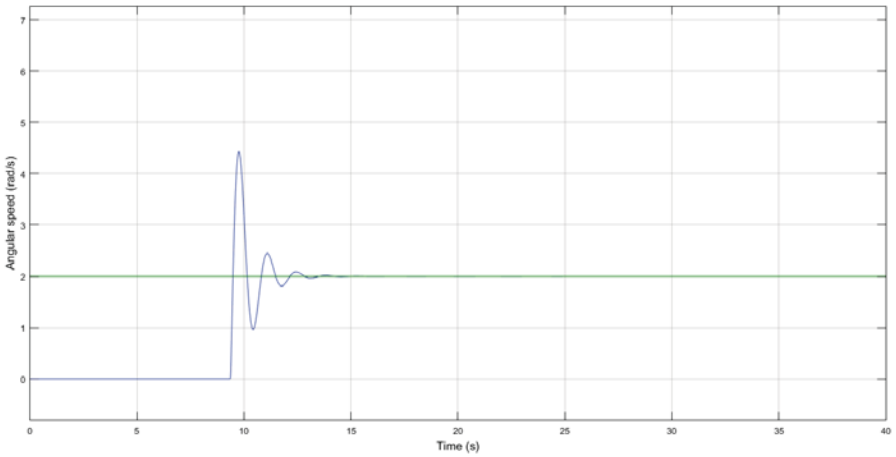

Figure 2.10: Simulation with Coulomb friction coefficient $\mu = 0.48$

By simulating the system increasing the breakaway friction coefficient from 0.5 to 0.6, with all the parameters shown in tab. 2.4, one can see that with the increase of the breakaway friction coefficient, the stick phase of the system increases when compared to the case shown in fig. 2.9, as more torque is needed to break loose the bit, and this bigger torque takes longer to be accumulated on the drillstring.

Parameter	**Value**	**Unit**
Breakaway friction coefficient (μ_{brk})	0.6	–
Coulomb friction coefficient (μ_c)	0.47	–
Normal force on Bit (N_f)	26	N
Viscous friction coefficient (b)	0.001	$\frac{Nm}{rad/s}$

Table 2.4: Friction parameters

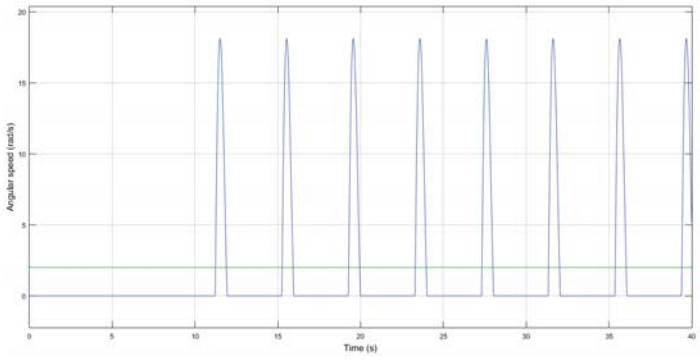

Figure 2.11: Simulation with Coulomb friction coefficient $\mu = 0.6$

Following, we compare how the viscous friction can affect the stick-slip. Figure 2.12 shows the simulation with parameters shown in tab. 2.2 as a base case.

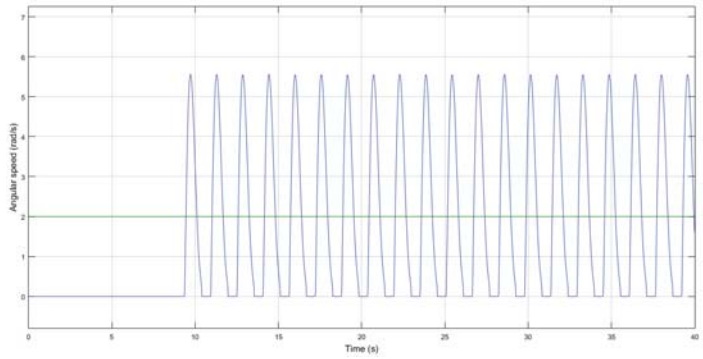

Figure 2.12: Simulation with viscous friction coefficient $b = 0.001$

We then modify the viscous friction coefficient to $\mu = 0.005$ with the other parameters shown in tab. 2.5. One can see that this increase of the viscous friction coefficient avoids the stick-slip of the system for the same set of parameters, even though it doesn't eliminate the torsional oscillations and over speed on the bit.

Parameter	**Value**	**Unit**
Breakaway friction coefficient (μ_{brk})	0.5	–
Coulomb friction coefficient (μ_c)	0.47	–
Normal force on Bit (N_f)	26	N
Viscous friction coefficient (b)	0.005	$\frac{Nm}{rad/s}$

Table 2.5: Friction parameters

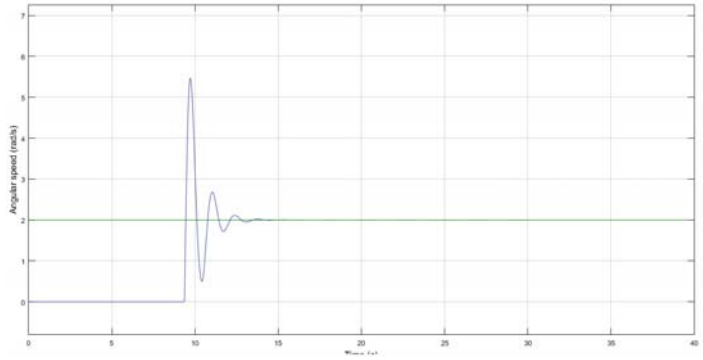

Figure 2.13: Simulation with viscous friction coefficient $b = 0.005$

Results presented in this section shows that changing, even slightly, the friction coefficients can modify the stick slip behavior or even eliminate the stick slip. This is an important conclusion about how the friction parameters

influence the formation of stick-slip motion, and gives a direction about a possibility to develop methods and devices to avoid stick-slip oscillations.

In the next chapter some control formulations will be presented and its simulation results analyzed. These controllers are first tested in a two cart problem, to validate its results with literature, and then simulations are made with the 20 DOF model of the drillstring, where the output is the angular velocity of J_1 and the top drive motor speed is the controlled parameter.